

TOPOLOGICAL BIREFRINGENCE OF OPTICAL VORTICES IN INHOMOGENEOUS MEDIA

A.V. Volyar, V.Z. Zhilaitis, V.G. Shvedov, M.S. Soskin, and T.A. Fadeeva

Simferopol' State University

Received August 3, 1998

The results of theoretical and experimental study of propagation and transformation of circularly symmetrical fields of TE vortices and linearly polarized azimuthally symmetric fields of TE and TM modes in a locally isotropic inhomogeneous medium of low-mode optical fibers are presented. The propagation constant for CV vortices as well as for TE and TM modes, as a scalar approximation of the wave equation, is shown to be fourfold degenerated with respect to topological charge and spirality. As a result of spin-orbital interaction in the eigenmodes field, the line of the propagation constant splits into four lines. The distance between the lines is equal to polarization corrections $\delta\beta$ to fields of eigenmodes. The form of the spin-orbit interaction operator is presented. The action of the operator onto fields of CV vortices, TE- and TM-modes is shown to induce topological birefringence in the locally isotropic medium of optical fibers. The birefringence manifests itself experimentally in the joint Rytov–Magnus effect.

1. INTRODUCTION

Optical vortices can carry both orbit and spin angular momenta in a free space. For a circularly polarized paraxial light beam with spirality σ_z (circulation direction of circular polarization) and topological charge l , the ratio of the z -component of the angular momentum flow to the z -component of energy flow equals^{1,2}

$$(l + \sigma_z)/\omega \quad (1)$$

(ω is frequency; $\sigma_z = \pm 1$). It means that a light beam with $l = +1$ and $\sigma_z = +1$, interacting with a substance, can transfer double angular momentum, and a beam with $l = +1$ and $\sigma_z = -1$ (or $l = -1$ and $\sigma_z = +1$) has no angular momentum.

It is evident that there is no interaction between orbit and spin parts of the angular momentum in a free space. However, spin-orbit interaction can arise in an optical vortex if propagation of a wave is bounded by a potential well (e.g., inhomogeneous medium or optical fiber). What physical properties correspond to the result of spin-orbit interaction in a light wave that is spread through optical fiber? On the one hand, it is well-known that, in spectra of substance atoms, this interaction splits energy levels³ and forms a fine structure of the spectrum. However, in a light wave, with comparatively small intensity, the energy spectrum is strictly determined by the spectrum of the radiation source. On the other hand, it is rightful to suppose that interaction of the orbit and spin parts of

the angular momentum causes a certain non-holonomic perturbation of the electromagnetic field. Note that non-holonomic perturbation of the field results in the topological phase γ_T additional to the dynamic phase ϕ_D of the wave.⁴ Since the phase γ_T depends on the direction of path-tracing in the parameter space (in our case, on the sign of the topological charge) and on the direction of rotation of circular polarization, this topological addition to the phase of the light wave will “split” the propagation constant of the eigenmode of a “non-disturbed” optical fiber.

The aim of this paper is to study physical nature of the phenomenon of splitting of the polarization

correction $\delta\beta$ to the scalar propagation constant $\tilde{\beta}$ for fields of optical CV vortices, TE and TM modes of a low-mode ($l \sim 1$) fiber.

The second section of the paper presents the zero polarization correction to the scalar propagation constant. The correction is responsible for the “level split” as the mean value of the operator of spin-orbit interaction in the field of optical vortices. In the third and the fourth sections the polarization correction is considered as the topological Berry phase of the field. The phase arises as a result of precession of the Poynting vector. The problem of topological birefringence of a locally isotropic low-mode fiber as a result of spin-orbit interaction is discussed in the fifth section. Particular examples demonstrate that the Rytov–Vladimirskii effect^{6,7} and the optical Magnus effect^{8,9} are exhibition of spin-orbit interaction.

2. THE OPERATOR OF SPIN-ORBIT INTERACTION

Let us use the formal correspondence between the wave equation of light in a inhomogeneous medium and the Schrödinger equation, just as it is made in Refs. 10–12, and find out the operator that corresponds to the observed value of the polarization correction $\delta\beta$.

Let us write the vector wave equation for light in an inhomogeneous medium¹³

$$[\nabla_{\perp}^2 + n^2(r) k^2 - \beta^2] \mathbf{e}_{\perp} = -\nabla_{\perp} [\mathbf{e}_{\perp} \nabla_{\perp} \ln n^2(r)], \quad (2)$$

where the index \perp points to lateral components of the vectors, β is the propagation constant of eigenmodes in an optical fiber with a gradient profile of the refractive index,

$$n^2(r) = n_{co}^2 [1 - 2 \Delta f(r)], \quad (3)$$

where Δ is the height of the profile, $f(r)$ is the profile function.

If the refractive indices of the core n_{co} and cladding n_{cl} are close, i.e., the parameter Δ is small, the equation (2) can be written in the form¹³

$$[\nabla_{\perp}^2 + n^2(r) k^2 - \tilde{\beta}^2] \tilde{\mathbf{e}}_{\perp} = 0 \quad (4)$$

as a first approximation of the perturbation theory.

The equation (4) does not take into account polarization properties of the field and, for this reason, it is called a scalar wave equation. Vector properties of fields are taken into account by transformation of the scalar amplitude of the field $\tilde{\mathbf{e}} \rightarrow \mathbf{e}$ and the propagation constant $\tilde{\beta} \rightarrow \beta$, so $\beta = \tilde{\beta} + \delta\beta$, where $\delta\beta$ is the polarization correction.

The solution of the scalar wave equation (4) for the fields of axially symmetric fibers in a linearly polarized basis was presented in Ref. 13. The spectrum of eigenfunctions and eigenvalues of this equation was presented in Ref. 14 in the form of optical vortices. They can be represented as:

1) directed circularly polarized $CV_{\sigma l, m}^{\kappa\sigma}$ vortices which are subdivided into

– *stable, topologically homogeneous vortices:*

$$CV_{\sigma l, m}^{\sigma} = HE_{l+1, m}^{\text{even}} + i\sigma HE_{l+1, m}^{\text{odd}}$$

$$(\kappa = +1, l \geq 1, \sigma = \pm 1, \beta_1 = \tilde{\beta} + \delta\beta_1),$$

they are denoted as $|+l; +1\rangle$ or $|-l; -1\rangle$;

– *stable, topologically inhomogeneous vortices:*

$$CV_{\sigma l, m}^{-\sigma} = EH_{l-1, m}^{\text{even}} + i\sigma EH_{l-1, m}^{\text{odd}}$$

$$(\kappa = -1, l > 1, \sigma = \pm 1, \beta_2 = \tilde{\beta} + \delta\beta_2),$$

denoted as $|+l; -1\rangle$ or $|-l; +1\rangle$;

2) azimuthally symmetric linearly polarized *TM* and *TE* modes which can be united in *unstable, topologically inhomogeneous vortices*

$$IV_{\sigma, m}^{-\sigma} = TM_{0m} + i\sigma TE_{0m}$$

$$(\kappa = -1, l = 1, \sigma = \pm 1),$$

denoted as $|+1; -1\rangle$ or $|-1; +1\rangle$.

Let us find the expression for the polarization correction $\delta\beta$. By the equations (2) and (4) one can obtain the relations (below we omit the index \perp)

$$(\beta^2 - \tilde{\beta}^2) \mathbf{e}^* \tilde{\mathbf{e}} + \mathbf{e}^* \nabla^2 \tilde{\mathbf{e}} - \tilde{\mathbf{e}} \nabla^2 \mathbf{e}^* = \tilde{\mathbf{e}} \nabla (\mathbf{e}^* \nabla \ln n^2), \quad (5)$$

$$(\beta^2 - \tilde{\beta}^2) \mathbf{e} \tilde{\mathbf{e}}^* + \mathbf{e} \nabla^2 \tilde{\mathbf{e}}^* - \tilde{\mathbf{e}}^* \nabla^2 \mathbf{e} = \tilde{\mathbf{e}}^* \nabla (\mathbf{e} \nabla \ln n^2). \quad (6)$$

Let us take into account that $\beta^2 - \tilde{\beta}^2 = (\beta + \tilde{\beta}) \times (\beta - \tilde{\beta}) \approx 2\tilde{\beta} \delta\beta$.¹³ Then, summing Eqs. (5) and (6) and integrating over the cross section of the fiber S , we obtain

$$\delta\beta = A \int_S \{(\tilde{\mathbf{e}}^* \nabla^2 \mathbf{e} - \mathbf{e} \nabla^2 \tilde{\mathbf{e}}^*) + (\tilde{\mathbf{e}} \nabla^2 \mathbf{e}^* - \mathbf{e}^* \nabla^2 \tilde{\mathbf{e}}) + [\tilde{\mathbf{e}}^* \nabla (\mathbf{e} \nabla \ln n^2) + \tilde{\mathbf{e}} \nabla (\mathbf{e}^* \nabla \ln n^2)]\} dS, \quad (7)$$

where $A^{-1} = \frac{2V}{\rho \sqrt{2} \Delta} \int_S (\tilde{\mathbf{e}}^* \mathbf{e} + \tilde{\mathbf{e}} \mathbf{e}^*) dS$ is the normalizing factor.

Profile height of the refractive index Δ is a small parameter, so $\Delta \rightarrow 0$ in the case of the scalar wave equation (4). To take into account polarization corrections induced by the right side of the vector wave equation (2), let us represent the electric field \mathbf{e} as a series with respect to orders of the infinitesimal of Δ (see Ref. 13)

$$\mathbf{e} = \tilde{\mathbf{e}}|_{\Delta=0} + \Delta \mathbf{e}^{(1)} + \Delta^2 \mathbf{e}^{(2)} + \dots \quad (8)$$

Let us restrict ourselves by two first terms in Eq. (8). Then we must simultaneously restrict ourselves by the first term in the expansion of the value $\nabla \ln n^2(r)$, where $n(r)$ is given by the expression (3): $\nabla \ln n^2 \approx -2 \Delta \nabla f$. The polarization correction (7) can be represented in the form

$$\delta\beta = \delta\tilde{\beta} + 2\Delta^2 A \iint_{S_{\infty}} (\mathbf{e}^{(1)} \nabla f \nabla \tilde{\mathbf{e}}^* + \mathbf{e}^{(1)*} \nabla f \nabla \tilde{\mathbf{e}}) dS, \quad (9)$$

where the orders of the infinitesimal values $\delta\tilde{\beta}$ and $\delta\beta^{(1)}$ are Δ and Δ^2 , respectively.

Let us first consider the operator representation of the polarization correction $\delta\tilde{\beta}$ to the zero order field $\tilde{\mathbf{e}}$.

One can demonstrate that $\tilde{e}_k^* \partial_k f \partial_i \tilde{e}_i = \tilde{e}_k \partial_k f \partial_i \tilde{e}_i^*$ for all eigenfields of the optical fiber. Here the indices i and k take on the values x and y , $\partial_i = \frac{\partial}{\partial x_i}$ and the repeating indices mean summation. In this case, for the polarization correction we obtain

$$\delta\tilde{\beta} = 2\Delta A \iint_S \tilde{e}_i^* \partial_i f \partial_k \tilde{e}_k dS, \quad (10)$$

where $\mathbf{e} \approx \tilde{\mathbf{e}}$ is assumed. Let us represent the integrand of Eq. (10) in the operator form

$$\begin{aligned} \tilde{e}_i^* \partial_i f \partial_k \tilde{e}_k &= (\tilde{e}_x^*, \tilde{e}_y^*) \times \\ &\times \begin{pmatrix} \partial_x f \partial_x & \partial_x f \partial_y \\ \partial_y f \partial_x & \partial_y f \partial_y \end{pmatrix} \begin{pmatrix} \tilde{e}_x \\ \tilde{e}_y \end{pmatrix} = \langle \tilde{\mathbf{e}} | \hat{\mathbf{V}} | \tilde{\mathbf{e}} \rangle. \end{aligned} \quad (11)$$

and decompose the matrix differential operator with respect to the Pauli matrices

$$\hat{\mathbf{V}} = \hat{\sigma}_0 \hat{\mathbf{V}}_0 + \hat{\sigma}_1 \hat{\mathbf{V}}_1 + \hat{\sigma}_2 \hat{\mathbf{V}}_2 + \hat{\sigma}_3 \hat{\mathbf{V}}_3,$$

where

$$\begin{aligned} \hat{\mathbf{V}}_0 &= \frac{1}{2} (\partial_x f \partial_x + \partial_y f \partial_y) = \frac{1}{2} \partial_r f \partial_r; \\ \hat{\mathbf{V}}_1 &= \frac{1}{2} (\partial_x f \partial_x - \partial_y f \partial_y) = \\ &= \frac{1}{2} \partial_r f \left(\cos 2\varphi \partial_r - \frac{1}{r} \sin 2\varphi \partial_\varphi \right); \\ \hat{\mathbf{V}}_2 &= \frac{1}{2} (\partial_x f \partial_y + \partial_y f \partial_x) = \\ &= \frac{1}{2} \partial_r f \left(\sin 2\varphi \partial_r + \frac{1}{r} \cos 2\varphi \partial_\varphi \right); \\ \hat{\mathbf{V}}_3 &= \frac{i}{2} (\partial_x f \partial_y - \partial_y f \partial_x) = \frac{i}{2r} \partial_r f \partial_\varphi. \end{aligned} \quad (12)$$

Using the cylindrical coordinate system, we restrict ourselves by the case of an axially symmetric fiber ($\partial_\varphi f = 0$). It is convenient to represent the operator $\hat{\mathbf{V}}$ in the form

$$\hat{\mathbf{V}} = \frac{1}{2\rho^2} \frac{\partial f}{\partial r} (\hat{\mathbf{D}} + \hat{\mathbf{T}} \hat{\mathbf{D}}),$$

where

$$\begin{aligned} \hat{\mathbf{D}} &= \hat{\sigma}_0 \frac{\partial}{\partial R} + \frac{i}{R} \hat{\sigma}_3 \frac{\partial}{\partial \varphi}; \\ \hat{\mathbf{T}} &= \hat{\sigma}_1 \cos 2\varphi + \hat{\sigma}_2 \sin 2\varphi = \\ &= \begin{pmatrix} \cos 2\varphi & \sin 2\varphi \\ \sin 2\varphi & -\cos 2\varphi \end{pmatrix}_L = \begin{pmatrix} 0 & e^{-i2\varphi} \\ e^{i2\varphi} & 0 \end{pmatrix}_C. \end{aligned} \quad (13)$$

The index L means that the matrix operators are represented in a linearly polarized basis. The index C points to a circularly polarized basis.

The form (13) is similar to the operator of spin-orbit interaction for electrons in a cylindrically

symmetric field. The mean value of the physical value of the operator $\hat{\mathbf{V}}$ is equal to the polarization correction $\delta\tilde{\beta}$. The operator $\hat{\mathbf{D}}$ includes the components that are similar to the operator of contact interaction $\hat{\mathbf{K}} = \hat{\sigma}_0 \frac{\partial}{\partial R}$ and spin-orbit interaction $\hat{\mathbf{S}} = \frac{i}{R} \hat{\sigma}_3 \frac{\partial}{\partial \varphi}$ for an electron in a hydrogen atom.¹⁵ The properties of the spin-orbit interaction operator are presented in Table I.

For instance, for a fiber with parabolic profile of the refractive index, the correction is

$$\delta\tilde{\beta} = -\kappa (l + \kappa) (\sqrt{2\Delta})^3 / (2\rho V). \quad (14)$$

Note that topological properties of low-mode fibers connected with the non-holonomic Berry phase are caused by action of the operator $\hat{\mathbf{T}}$ on the fields of CV vortices (see Table I).

Action of the operators $\hat{\mathbf{D}}$ and $\hat{\mathbf{T}} \hat{\mathbf{D}}$ on circularly polarized CV vortices significantly differs from their action on linearly polarized azimuthally symmetric fields of TE and TM modes. The operator $\hat{\mathbf{D}}$ transforms the radial distribution of the field: $F_l(R) \Rightarrow G_l^{-\kappa}(R)$, where $G_l^{-\kappa}(R) = \frac{dF_l}{dR} - \kappa \frac{l}{R} F_l$. The matrix $\hat{\mathbf{T}}$ can be represented as a product of the Pauli matrix $\hat{\sigma}_1$ and operator of rotation by an angle 2φ

$$\hat{\mathbf{T}} = \hat{\sigma}_1 \hat{\mathbf{R}}(2\varphi) = \begin{pmatrix} 1 & 0 \\ 0 & -1 \end{pmatrix} \begin{pmatrix} \cos 2\varphi & \sin 2\varphi \\ -\sin 2\varphi & \cos 2\varphi \end{pmatrix}. \quad (15)$$

The rotation operator $\hat{\mathbf{R}}$ transforms the value of the topological charge in the following way: $l \Rightarrow l + 2\kappa$. The matrix $\hat{\sigma}_1$ changes the direction of circulation by the opposite one: $\sigma^+ \Leftrightarrow \sigma^-$. Action of the operator $\hat{\mathbf{T}} \hat{\mathbf{D}}$ on the fields $\tilde{\mathbf{e}}$ for CV vortices transforms them into orthogonal mode states. So, a contribution to the polarization correction $\delta\tilde{\beta}$ is given only by the operator $\hat{\mathbf{D}}$ which does not change the state of field polarization and does not transform the field phase. It is different from action of the operators $\hat{\mathbf{D}}$ and $\hat{\mathbf{T}} \hat{\mathbf{D}}$ upon the fields of TE and TM modes. In this case, both the parts of the operator $\hat{\mathbf{V}}$ bring a contribution in the field variation. Therefore, in an "overradiated" field of TE and TM modes, both the field and phase are varied. This difference in action of the operator \mathbf{V} on polarization of fields of CV vortices and TE, TM modes indicates the presence of two physical processes: circular birefringence for the field of CV vortices and linear birefringence for TE and TM modes.

TABLE I. Transformation of fields and their propagation constants under the action of the operator of spin-orbit interaction.

		$\begin{matrix} \kappa = +1 & l \geq 1 \\ \kappa = -1 & l > 1 \end{matrix} \quad \sigma = \pm 1$	$\kappa = -1 \quad l = 1$	$\kappa = -1 \quad l = 1$
		$C V_{\sigma l}^{\kappa \sigma}$	TM	TE
$ \tilde{\mathbf{e}}\rangle$	e_x	$\frac{1}{\sqrt{2}} F_l e^{i\sigma l \varphi}$	$F_l \cos \varphi$	$F_l \sin \varphi$
	e_y	$\frac{i\kappa \sigma}{\sqrt{2}} F_l e^{i\sigma l \varphi}$	$F_l \sin \varphi$	$-F_l \cos \varphi$
$\hat{\mathbf{D}} \tilde{\mathbf{e}}\rangle$	e_x	$\frac{1}{\sqrt{2}} G_l^{-\kappa} e^{i\sigma l \varphi}$	$G_l^+ \cos \varphi$	$G_l^+ \sin \varphi$
	e_y	$\frac{i\kappa \sigma}{\sqrt{2}} G_l^{-\kappa} e^{i\sigma l \varphi}$	$G_l^+ \sin \varphi$	$-G_l^+ \cos \varphi$
$\hat{\mathbf{T}} \hat{\mathbf{D}} \tilde{\mathbf{e}}\rangle$	e_x	$\frac{1}{\sqrt{2}} G_l^{-\kappa} e^{i\sigma(l+2\kappa)\varphi}$	$G_l^+ \cos \varphi$	$-G_l^+ \sin \varphi$
	e_y	$\frac{i\kappa \sigma}{\sqrt{2}} G_l^{-\kappa} e^{i\sigma(l+2\kappa)\varphi}$	$G_l^+ \sin \varphi$	$G_l^+ \cos \varphi$
$a \langle \tilde{\mathbf{e}} \frac{\partial f}{\partial R} \hat{\mathbf{D}} \tilde{\mathbf{e}}\rangle$		$I_l^{-\kappa}$	I_l^+	I_l^+
$a \langle \tilde{\mathbf{e}} \frac{\partial f}{\partial R} \hat{\mathbf{T}} \hat{\mathbf{D}} \tilde{\mathbf{e}}\rangle$		0	I_l^+	$-I_l^+$
$\delta \tilde{\beta}$		$I_l^{-\kappa}$	$2 I_l^+$	0
$\delta \beta \quad (f = R^2)$		$-\kappa (l + \kappa) \frac{(\sqrt{2\Delta})^3}{2\rho V}$	0	0

$$a = \frac{(\sqrt{2\Delta})^3}{4\rho V} \frac{1}{\langle \tilde{\mathbf{e}} | \tilde{\mathbf{e}} \rangle}; \quad \delta \tilde{\beta} = \frac{(\sqrt{2\Delta})^3}{4\rho V} \frac{\langle \tilde{\mathbf{e}} | \frac{\partial f}{\partial R} (\hat{\mathbf{D}} + \hat{\mathbf{T}} \hat{\mathbf{D}}) | \tilde{\mathbf{e}} \rangle}{\langle \tilde{\mathbf{e}} | \tilde{\mathbf{e}} \rangle}; \quad I_l^{-\kappa} = \frac{(\sqrt{2\Delta})^3}{4\rho V} \int_0^\infty \frac{\partial f}{\partial R} F_l G_l^{-\kappa} R dR / \int_0^\infty F_l^2 R dR.$$

Nevertheless the eigenfunctions of the operator $\hat{\mathbf{V}}$ do not coincide with the value of the correction field $\mathbf{e}^{(1)}$. Let us study the physical nature of the polarization correction $\delta \tilde{\beta}$.

3. TOPOLOGICAL PHASE AND POLARIZATION CORRECTION

As was demonstrated in Ref. 4, adiabatic cyclic variation of parameters of the wave function of a microparticle leads to appearance of the non-holonomic topological phase γ_T . The phase γ_T is characterized by the result of *parallel displacement* of the state vector along a closed curve in the configuration space and arises due to *action of a non-holonomic constraint*, in particular, due to propagation of a transversal light wave in an inhomogeneous medium.

In optics, the topological phase arises as a rule in wave processes accompanied by variations of the polarization state or spin direction with respect to the z axis. In the electrodynamics representation such a process corresponds, for instance, to wave passing

through a ream of anisotropic slabs (Pancharatnam phase¹⁶) or in propagation of light by a non-flat ray trajectory (Rytov-Vladimirskii phase^{6,7}). Accumulation of the topological phase can also be manifested due to variation of the lateral structure of a laser beam in an astigmatic mode converter.¹⁷ This variety of topological phases is systematized in Ref. 4 and called the Berry phase.¹⁸

However, propagation of eigenvortices through an optical fiber is not connected with variations of any explicit parameters of a wave. Nevertheless the presence of the p_φ -component of the energy flow causes precession of the Poynting vector around the z axis. The energy flow can be characterized by "force" lines. The "force" lines of the Poynting vector (Fig. 1) for homogeneous and inhomogeneous vortices take the form of spiral trajectories. The energy flow of homogeneous $CV_{\sigma l}^{\sigma}$ vortices contains a topologically homogeneous field of helices (Fig. 1a). For inhomogeneous $CV_{\sigma l}^{-\sigma}$ vortices, the field of the Poynting vector contains two types of helical trajectories differing in pitch and torsion sign (Fig. 1b) and separated by a family of straight lines.

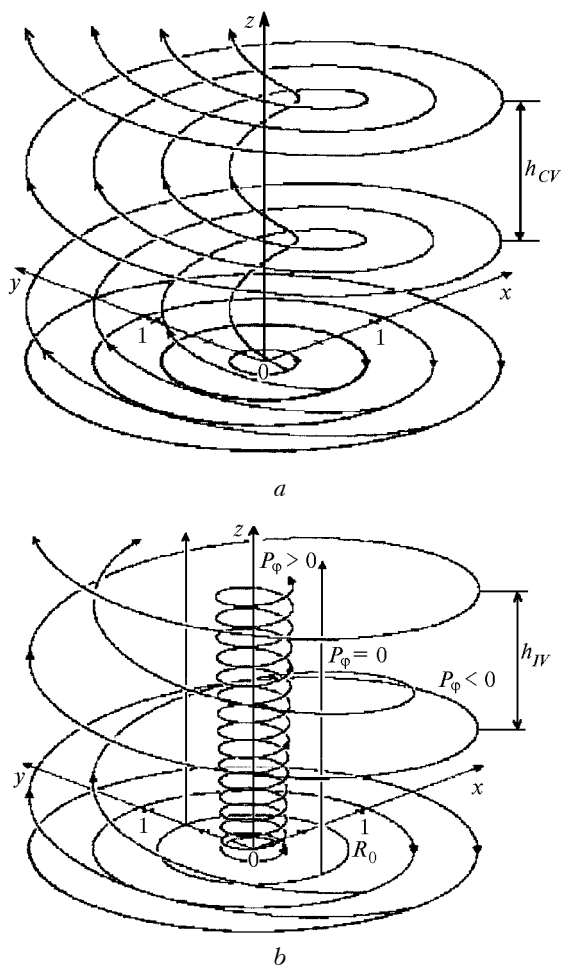


FIG. 1. Lines of energy flow: (a) stable topologically homogeneous CV vortex ($\kappa = +1, l = 1$); (b) unstable topologically inhomogeneous IV vortex ($\kappa = -1, l = 1$).

3.1. Homogeneous vortices of a parabolic fiber

Let us consider the process of accumulation of the topological phase γ_T in the field of a homogeneous $CV_{\sigma l}^{\sigma}$ vortex in an optical fiber with a parabolic profile of the refractive index $n^2(R) = n_{co}^2(1 - 2\Delta R^2)$. As seen from Fig. 1a, the helix pitch h_1 is the same for all the lines of the energy flow of a $CV_{\sigma l}^{\sigma}$ vortex and equals

$$h_1 = 2\pi\rho/\sqrt{2\Delta}. \tag{16}$$

The helix pitch h_1 is determined only by the full radius of the fiber ρ and profile height of the refractive index Δ . Equation (16) describes only weakly directing fibers. So it is not surprising that the helix pitch h_1 coincides with the pitch of the spiral trajectory of rays in a multimode light guide in the paraxial approximation of geometrical optics (Eq. (2.38) in Ref. 13).

It means that the Poynting vector \mathbf{P} executes a precession motion along the propagation axis z during propagation of a homogeneous CV vortex. Let us perform parallel displacement of the electric vector \mathbf{e} on

a sphere along a “stream” line of the vector \mathbf{P} (Ref. 5) by an angle φ and, after easy calculations, obtain the topological phase γ_T

$$P_T = \varphi (1 - P_z/P), \tag{17}$$

where $P^2 = P_\varphi^2 + P_r^2 + P_z^2$; φ is the azimuth angle of rotation of the origin of the moving frames at the “stream” line of the vector \mathbf{P} . The specific topological phase (phase per unity of trajectory length in the phase space) for homogeneous $CV_{\sigma l}^{\sigma}$ vortices can be written in the form

$$\begin{aligned} \theta_1 &= \frac{\partial\gamma_T}{\partial z} = \left(1 - \frac{P_z}{P}\right) \frac{\partial\varphi}{\partial z} = \frac{2\pi}{h_1} \left(1 - \frac{P_z}{P}\right) = \\ &= \frac{\sqrt{2\Delta}}{\rho} \left(1 - \frac{1}{\sqrt{1 + 2\Delta R^2}}\right) = \frac{(\sqrt{2\Delta})^3 R^2}{2\rho} - \\ &- \frac{3(\sqrt{2\Delta})^5 R^4}{8\rho} + \frac{5(\sqrt{2\Delta})^7 R^6}{16\rho} - \dots \end{aligned} \tag{18}$$

In a multimode fiber, the direction of energy propagation can be related to the direction of the ray trajectory as a certain approximation.¹³ However, the “stream” lines of the vector \mathbf{P} cannot be identified with ray trajectories for a low-mode fiber: eigenmodes are spread along the z axis. At the same time, energy flow in a fiber is not homogeneous in the lateral section and is characterized by the module of \mathbf{P} . Let us find the mean value of θ_1 with respect to the state $p = |\mathbf{p}|$, restricting ourselves by the series’ term of order $(2\Delta)^{3/2}$ in Eq. (18)

$$\begin{aligned} \langle\theta_1\rangle &= \frac{\int_{\theta_1} \theta_1 P d\theta_1}{\int_{\theta_1} P d\theta_1} \approx - \frac{(\sqrt{2\Delta})^3}{2\rho V} (l + 1), \\ (\kappa = +1). \end{aligned} \tag{19}$$

The obtained value of the specific topological phase $\langle\theta_1\rangle$ exactly coincides with the polarization correction $\delta\beta_1$ to the propagation constant of the even and odd me_{l+1} modes (Tables 14.1 and 14.2, Ref. 13) by use of which one can form a $CV_{\sigma l}^{\sigma}$ vortex.^{19,20} It coincides also with the mean value of the operator of spin-orbit interaction $\hat{\mathbf{V}}$ (Eq. (14)).

3.2. Inhomogeneous vortices of a parabolic fiber

Let us obtain the topological phase acquired by an inhomogeneous $CV_{\sigma l}^{-\sigma}$ vortex. One can demonstrate¹⁴ that the full flow of the angular momentum for $IV_{\sigma}^{-\sigma}$ vortices is zero: $l_z(IV) = 0$. This is a consequence of topological inhomogeneity of “stream” lines of the vector \mathbf{P} for IV vortices (see Fig. 1b). Such a structure of the vector \mathbf{P} also leads to inhomogeneous character

of the topological phase θ_2 and, as a consequence, causes divergence of the integrals in Eq. (19). To avoid this difficulty, let us consider a significantly multimode fiber with a waveguide parameter $V \rightarrow \infty$. The spiral pitch of the $CV_{\sigma l}^{-\sigma}$ vortex is

$$h_2 = \frac{2\pi\rho}{\sqrt{2\Delta}} \frac{1}{1 - R_0^2/R^2}, \quad R_0 = \sqrt{\frac{2l}{V}}. \quad (20)$$

As seen from Eq. (20), the characteristic radius $R_0 \rightarrow 0$ as $V \rightarrow \infty$. In this case, two singularities for $R = R_0$ and $R = 0$ superpose at the fiber axis and annihilate, and Eq. (20) coincides with Eq. (16).

Analysis of Eq. (20) demonstrates that the precession direction of the Poynting vector of an inhomogeneous vortex depends on the spiral radius R . As seen in Fig. 1b, precession directions are opposite at the parts with $R < R_0$ and $R > R_0$.

Since the fields of a $CV_{\sigma l}^{-\sigma}$ vortex can be composed by two $e m_{l-1}$ modes^{19,20} by substitution of the index $l+1$ instead of $l-1$ in Eq. (19), we come to the expression for the specific topological phase of inhomogeneous CV vortices

$$\langle \theta_2 \rangle = (\sqrt{2\Delta})^3 / (2\rho V) (l-1), \quad (\kappa = -1). \quad (21)$$

The obtained expression for $\langle \theta_2 \rangle$ exactly coincides with the expression for the polarization correction $\delta\beta_2$ to the propagation constant of the even and odd $e m_{l-1}$ modes (Tables 14.1 and 14.2, Ref. 13) and with the mean value of the operator of spin-orbit interaction \hat{V} (see Eq. (14)). As follows from the form of Eqs. (19) and (21), the topological phase of directed vortices depends on two parameters: azimuth index l and index of spin-orbit connection κ . Such a separation of the indices l and κ indicates the presence of two processes in propagation of an optical vortex: directions of both orbit and spin angular momenta vary cyclically. As seen from Eq. (21), the topological phase $\langle \theta_2 \rangle$ vanishes for the IV vortex of a parabolic fiber. This result is directly connected with the fact that the z -component of the angular momentum of the IV vortex is zero due to opposite directions of the spin and orbit angular momenta.

Let us write Eqs. (19) and (21) in a form of temporal dimensional representation

$$\tau_l^\kappa = \frac{\rho^2}{c\Delta} \langle \theta_l^\kappa \rangle = -\kappa \frac{l+\kappa}{\omega n_{co}}. \quad (22)$$

The value τ_l^κ in Eq. (22) depends only on the parameters of the vortex field and is the proper time of the directed vortex of the optical fiber. It is easy to see that $\tau_l^\kappa < 0$ for homogeneous CV vortices, $\tau_l^\kappa > 0$ for inhomogeneous CV vortices, and $\tau_l^\kappa = 0$ for IV vortices.

Multiplying the numerator and denominator of Eq. (22) by the Planck constant \hbar , we obtain the quotient of the angular momentum of a photon $L =$

$= -\hbar (\kappa l + 1)$ to photon energy $E = \hbar \omega$. Thus, one can assume that the value τ_l^κ characterizes a certain proper time of a photon propagating in a potential field $U = n^2(R) = n_{co}^2 (1 - 2\Delta R^2)$.

In transition from one vortex to another, the proper time τ_l^κ is measured in quanta and can take negative values.

4. ANGULAR MOMENTUM OF DIRECTED VORTICES

One can demonstrate that the components of the Poynting vector \mathbf{P} for directed vortices has the form

$$P_r = 0, \quad P_\phi = -\kappa \sigma K F_l(R) G_l^{-\kappa}(R),$$

$$P_z = K (V/\sqrt{2\Delta}) F_l^2(R), \quad (23)$$

where $F_l(R)$ is the amplitude function of the field (in the case of a parabolic fiber),

$$F_l(R) = R^l \exp(-VR^2/2);$$

$$G_l^{-\kappa} = \frac{dF_l}{dR} - \kappa \frac{l}{R} F_l; \quad K = E_0^2 n_{co} \sqrt{\frac{\epsilon_0}{\mu_0}} \frac{\sqrt{2\Delta}}{V}.$$

Using Eq. (23), let us find the z -component of the angular momentum of the vortex per unity of fiber length

$$L_z = \rho^2 \iint_S m_z R dR d\phi, \quad (24)$$

where

$$m_z = -\frac{1}{c^2} r P_\phi =$$

$$= -\kappa \sigma \frac{K}{c^2} \rho F_l(R) R \left[\frac{dF_l(R)}{dR} - \kappa \frac{l}{R} F_l(R) \right]$$

is the density of the angular momentum. Comparing Eq. (24) with the expression (10) from Ref. 1, we find that the first term of the sum can be formally associated with the spin angular momentum, and the second term with the orbit angular momentum of the vortex. Dividing the obtained expression by the full energy flow in the z -direction, we have

$$t_{\sigma l}^{\kappa\sigma} = \sigma (l + \kappa) / \omega, \quad (25)$$

what well agrees with Eq. (1) up to the index of spin-orbit connection ($l \rightarrow \sigma l$, $\sigma \rightarrow \kappa\sigma$). Comparing Eqs. (1), (22), and (25), we see that time τ_l^κ describes the result of spin-orbit interaction in directed vortices of a parabolic fiber. Since Eq. (22) describes the

polarization correction to propagation constants of circular vortices, we find that spin-orbit interaction in directed vortices removes degeneration of the propagation constant $\tilde{\beta}_l$ by $\tilde{\beta}_l^+$ and $\tilde{\beta}_l^-$. This process is

similar to that of spin-orbit interaction splitting energy levels in atoms.³

The expression (25) is obtained for an arbitrary profile of the refractive index $n(R)$ and demonstrates that spin-orbit interaction is characteristic for all fibers with cylindrical symmetry. However, identity of Eqs. (22) and (25) is peculiar only to parabolic fibers. One can demonstrate that the proper time τ_l^{\times} in fibers with step-type profile of the refractive index for directed vortices near the interception is determined as

$$\tau_l^{\times=+1} \approx -2(l-1)/\omega, \quad \tau_l^{\times=-1} \approx 0. \quad (26)$$

It follows from Eq. (26) that the character of spin-orbit interaction in directed vortices depends on the shape of the potential well profile.

5. TOPOLOGICAL BIREFRINGENCE OF OPTICAL VORTICES

5.1. Historical references. Main equations

The ability of a locally isotropic layered medium to cause birefringence in the field of an optical wave is known for a long time as birefringence of a form.²¹ This linear birefringence is connected with difference in boundary conditions for normal and tangent components of the electric field. Later, analyzing propagation of polarized light rays through a locally isotropic nonuniform medium, Rytov⁶ and Vladimirskii⁷ noted that a light wave underwent circular birefringence.

However, circular anisotropy of the medium manifests itself differently for light waves with flat and not flat ray trajectories. For waves with a flat ray trajectory, birefringence does not arise. At the same time, waves propagating by helical trajectories acquire different phase velocities for right and left circular polarization.

As it was demonstrated in Sect. 2 and 3, physical nature of different response of a locally isotropic nonuniform medium to right and left circular polarization of a wave is connected with the topological phase of the field. Action of linear and circular birefringence on fields of significantly multimode fibers (splitting ray trajectories or wave caustics) was studied in Refs. 8, 9 and called topological birefringence. Analyzing distribution of light rays in a nonuniform medium on the base of VKB-method, the authors of Refs. 22 and 23 came to the conclusion that the value of circular birefringence of a nonuniform medium is $\delta n_C \sim (\lambda/a)$, and linear birefringence is $\delta n_L \sim (\lambda/a)^2$, (λ is wavelength, a is the characteristic size of non-homogeneity).

It should be expected that the processes of birefringence must be most clearly seen in optical fibers due to uniquely long length of wave interaction with locally isotropic nonuniform medium of the fiber.

Differences in velocities of proper waves in analysis of solutions of Maxwell's equations are represented by a spectrum of propagation constants, and the variety of optical phenomena caused by differences in velocities of wave propagation in a fiber is known as the phenomenon of mode dispersion¹³ which is not connected with a special anisotropic response of the inhomogeneous medium.

Nevertheless, the propagation constant of each eigenmode can be decomposed into a scalar part $\tilde{\beta}_l$ (l is the azimuth index characterizing symmetry properties of the field) and a certain correction $\delta\beta_l^{\times}$ (\times is the index of spin-orbit connection) characterizing the polarization properties of the field.¹³

One can separate the mode dispersion as a phenomenon connected with the difference of scalar propagation constants $\tilde{\beta}_l$ from polarization effects splitting the "line" $\tilde{\beta}_l$ into a fine structure which is determined by the correction $\delta\beta_l^{\times}$. The polarization correction $\tilde{\delta\beta}$ is represented in Sect. 2 as the mean value of the physical value of operator $\hat{\mathbf{V}}$ of spin-orbit interaction (see Eq. (13)). In our opinion, it is spin-orbit interaction that causes birefringence of waves in a locally isotropic medium.

In this section we present the results of theoretical study of both separate and joint manifesting of circular and linear birefringence of optical vortices in low-mode fibers.

As seen from Table I, polarization correction $\tilde{\delta\beta}$ for TE and TM modes of a parabolic fiber is zero ($\tilde{\delta\beta}_{TE} = \tilde{\delta\beta}_{TM} = 0$). However, this does not mean that polarization correction $\delta\beta^{(1)}$ to the correction field $\mathbf{e}^{(1)}$ in Eq. (9) also equals zero for these modes. The case is that the polarization correction of zero order was obtained as an approximation $\tilde{\mathbf{e}} \rightarrow \mathbf{e}$. However, the symmetry form of force lines of a TE mode (Table III) excludes additional field distortion connected with the polarization correction: force lines of the field are normal to the curvature vector of the space of an axially symmetric fiber. The symmetry form of the field of a TM mode indicates a possible distortion of force lines which cause displacement of propagation constants of TE and TM modes.

On the other hand, the polarization correction $\tilde{\delta\beta}$ for CV vortices is larger than the correction $\delta\beta^{(1)}$ by an order of magnitude (see Eq. (9)). So the value $\tilde{\delta\beta}^{(1)}$ will not give significant distortions in the process of CV vortices propagation.

As seen from Eq. (9), to determine the value $\delta\beta^{(1)}$, it is necessary to obtain the form of the correction field $\mathbf{e}^{(1)}$. One can demonstrate that the correction field $\mathbf{e}^{(1)}$ satisfies the following equations¹³:

$$\left[\partial_R^2 + \frac{1}{R} \partial_R - \frac{1}{R^2} + \tilde{U}^2 - V^2 f + \frac{1}{R^2} \partial_\varphi^2 \right] e_r^{(1)} - \frac{2}{R^2} \partial_\varphi e_\varphi^{(1)} = 2 \partial_R f \partial_R \tilde{e}_r + 2 \partial_R^2 f \tilde{e}_r + \frac{4\rho V}{(\sqrt{2\Delta})^3} \delta\tilde{\beta} \tilde{e}_r, \tag{27}$$

$$\left[\partial_R^2 + \frac{1}{R} \partial_R - \frac{1}{R^2} + \tilde{U}^2 - V^2 f + \frac{1}{R^2} \partial_\varphi^2 \right] e_\varphi^{(1)} + \frac{2}{R^2} \partial_\varphi e_r^{(1)} = \frac{2}{R} \partial_R f \partial_\varphi \tilde{e}_r + \frac{4\rho V}{(\sqrt{2\Delta})^3} \delta\tilde{\beta} \tilde{e}_\varphi. \tag{28}$$

The form of the correction fields $e^{(1)}$ and values $\delta\beta^{(1)}$ for CV vortices, TE and TM modes as solutions of the equations (27), (28), and (9) is presented in Table II.

The condition $\delta\beta = 0$ is always satisfied for TE mode; however, $\delta\beta \neq 0$ for TM mode. For instance, in a fiber with a parabolic profile of the refractive index $f = R^2$, polarization corrections $\delta\tilde{\beta}$ equal zero both for

TE and TM mode: $\delta\tilde{\beta}_{TE, TM} = 0$. However, calculation that was performed on the base of data from Table II demonstrates that the value of the polarization correction $\delta\tilde{\beta}_{TM}^{(1)} \sim (\lambda/\rho)^{5/2}$. So propagation rates of TE and TM modes are different. It is the difference in propagation constants that is the main mechanism of linear birefringence of optical fibers whose value is $n_T = (\lambda/\rho)^3$. For instance, $V = 3.6$, $\Delta \sim 10^{-3}$, $\delta\beta \sim 10^{-1} \text{ m}^{-1}$ for a parabolic fiber with $\rho = 3.5 \mu\text{m}$, and the IV vortex breaks down at the length $\Lambda = 67 \text{ m}$. Earlier, the IV vortex in a parabolic fiber was believed to be stable.¹⁴

The term ‘‘linear birefringence’’ means that right circular polarization $\sigma = +1$ turn into left circular polarization in propagation of a wave. For instance, in a IV vortex, conversion of states

$$|+1, -1\rangle \Leftrightarrow |-1, +1\rangle$$

takes place at the half of the beating length.

TABLE II. Corrections to the electric fields and propagation constants for CV vortices, TE and TM modes of an optical fiber.

	$\kappa = +1 \quad l \geq 1$ $\kappa = -1 \quad l > 1 \quad \sigma = \pm 1$ CV $\frac{\kappa\sigma}{\sigma l}$	$\kappa = -1 \quad l = 1$ TM	$\kappa = -1 \quad l = 1$ TE
\tilde{e}_r	$\frac{1}{\sqrt{2}} \tilde{F}_l e^{i\sigma(l+2\kappa)\varphi}$	\tilde{F}_1	0
\tilde{e}_φ	$\frac{i\kappa\sigma}{\sqrt{2}} \tilde{F}_l e^{i\sigma(l+2\kappa)\varphi}$	0	\tilde{F}_1
$e_r^{(1)}$	$\frac{1}{\sqrt{2}} F_l^{(1)} e^{i\sigma(l+2\kappa)\varphi}$	$F_1^{(1)}$	0
$e_\varphi^{(1)}$	0	0	0
$\delta\beta^{(1)} (f = R^2)$	$-\kappa(l+1)(l+3\kappa) \frac{(\sqrt{2\Delta})^5}{2\rho V^2}$	$-2 \frac{(\sqrt{2\Delta})^5}{\rho V^2}$	0

For the profile $f = R^2$: $\tilde{F}_l = R^l \exp(-VR^2/2)$, $F_l^{(1)} = R^{l+2} \exp(-VR^2/2)$.

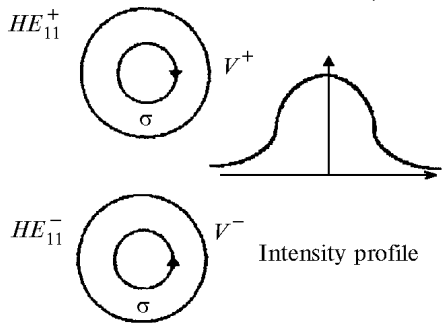
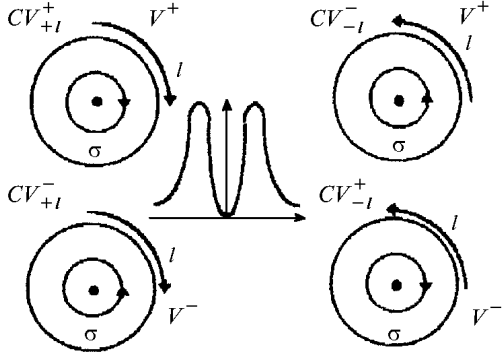
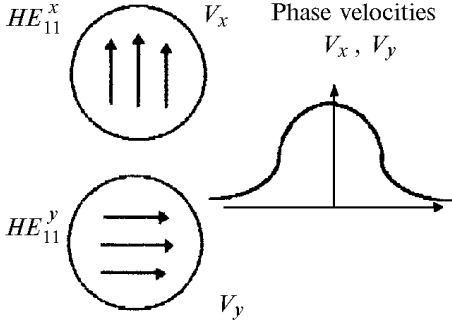
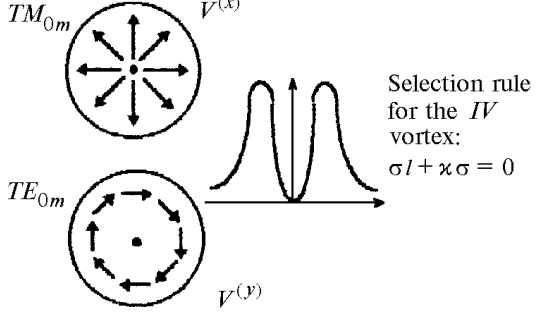
The contribution of the second term of Eq. (9) into the full polarization correction is very small for CV vortices. The main contribution is given by $\delta\tilde{\beta}$, which does not change polarization but is different for homogeneous and inhomogeneous CV vortices. So, CV vortices in the states $\{|+l, +1\rangle; |-l, -1\rangle\}$ and $\{|+l, -1\rangle; |-l, +1\rangle\}$ have different phase progressions at the same fiber length z . This phenomenon is identical to circular birefringence which is of more general character in this case (it is

described not only by the polarization basis but also by the topological charge) as compared with the classical analog in crystal optics.

Comparison of circular and linear birefringence of smooth fields of HE₁₁ modes and fields with phase and polarization singularities of CV vortices, TE and TM modes is presented in Table III.

Let us consider some particular cases of exhibitions of circular and linear birefringence in locally isotropic, non-disturbed multimode fibers.

TABLE III. Comparison of induced and topological birefringence of light in optical fibers.

Basic homogeneously polarized HE_{11} mode (induced birefringence)	Homogeneous and inhomogeneous CV vortices and azimuthally symmetric TE and TM modes
Circular birefringence	
<p style="text-align: center;">Phase velocities V^+, V^-</p>  <p style="text-align: center;">Intensity profile</p>	
<p>$l = 0, \sigma = \pm 1$ $HE_{11}^+ \Rightarrow \psi^+ \rangle = 0, +1\rangle,$ $HE_{11}^- \Rightarrow \psi^- \rangle = 0, -1\rangle$ eigenvalues: $\langle HE_{11}^+ \rangle \Rightarrow \tilde{\beta}_0 + \delta\beta^+$ $\langle HE_{11}^- \rangle \Rightarrow \tilde{\beta}_0 + \delta\beta^-$ in disturbance $\delta\beta^+ \neq \delta\beta^-$</p>	<p>$\psi^+ \rangle = \sigma l, \kappa \sigma \rangle$ homogeneous vortices $\kappa = +1, l \geq 1$ $CV_{+l}^+ \Rightarrow \psi^+ \rangle = l, +1\rangle,$ Selection rule: $CV_{-l}^- \Rightarrow \psi^+ \rangle = -l, -1\rangle$ $\sigma l + \kappa \sigma \neq 0$ inhomogeneous vortices $\kappa = -1, l > 1$ $CV_{+l}^- \Rightarrow \psi^- \rangle = l, -1\rangle$ $CV_{-l}^+ \Rightarrow \psi^- \rangle = -l, +1\rangle$ $\langle CV_{+l}^+ \rangle = \langle CV_{-l}^- \rangle \Rightarrow \tilde{\beta}_l + \delta\beta_l^+$ $\langle CV_{+l}^- \rangle = \langle CV_{-l}^+ \rangle \Rightarrow \tilde{\beta}_l + \delta\beta_l^-$</p>
Linear birefringence	
	 <p style="text-align: right;">Selection rule for the IV vortex: $\sigma l + \kappa \sigma = 0$</p>
<p>$HE_{11}^x: \psi \rangle \Rightarrow 0, +1\rangle + 0, -1\rangle$ $HE_{11}^y: \psi \rangle \Rightarrow 0, +1\rangle - 0, -1\rangle$ $\langle HE_{11}^x \rangle \Rightarrow \tilde{\beta}_0 + \delta\beta^x$ in disturbance $\langle HE_{11}^y \rangle \Rightarrow \tilde{\beta}_0 + \delta\beta^y$ $\delta\beta \neq \delta\beta^y$</p>	<p>$TM: \psi \rangle \Rightarrow -1, +1\rangle + 1, -1\rangle$ $TE: \psi \rangle \Rightarrow -1, +1\rangle - 1, -1\rangle$ $\langle TM \rangle \Rightarrow \tilde{\beta}_1 + \delta\beta_{TM}; \delta\beta_{TM} \neq 0$ $\langle TE \rangle \Rightarrow \tilde{\beta}_1 + \delta\beta_{TE}; \delta\beta_{TE} = 0$</p>

5.2. Circular birefringence. Rytov's effect and the optical Magnus effect

Let us consider propagation of superposition of homogeneous and inhomogeneous CV vortices²⁴ in a low-mode optical fiber.

$$LV_{\sigma l}^x = CV_{\sigma l}^{+\sigma} + CV_{\sigma l}^{-\sigma}, \tag{29}$$

$$CP_{\sigma l}^{\sigma} + CV_{+\sigma l}^{\sigma} + CV_{-\sigma l}^{\sigma}, \tag{30}$$

where $\kappa = +1$ for the first component and $\kappa = -1$ for the second one. Besides, the condition $l \neq 1$ must be

satisfied for inhomogeneous CV vortices. Using the expression for CV vortices, let us write the electric field of a linearly polarized $LV_{\sigma l}^x$ vortex in the form

$$\mathbf{e}_1(LV_{\sigma l}^x) = (\hat{\mathbf{x}} \cos \delta\beta_{21} z + \sigma \hat{\mathbf{y}} \sin \delta\beta_{21} z) \times F_l(R) \exp\{i\sigma l \varphi\} \exp\{i\tilde{\beta}' z\}, \quad (31)$$

where

$$\delta\beta_{21} = \frac{\delta\beta_2 - \delta\beta_1}{2}, \quad \tilde{\beta}' = \tilde{\beta} + \frac{\delta\beta_1 + \delta\beta_2}{2}.$$

It follows from Eq. (31) that the electric vector of linear polarization rotates by the angle

$$\psi = \sigma \delta\beta_{21} z = (2\pi/\lambda) \delta n_T z \quad (32)$$

during propagation of an LV vortex along the fiber. The angle is characterized by efficient birefringence

$$\delta n_T = (c^2 \Delta)/(n_{co} \rho^2 \omega^2) \sigma l. \quad (33)$$

The direction of rotation of the electric vector is determined by the sign of the topological charge. The expression (33) describes a waveguide analog of the Rytov–Vladimirskii effect^{6,7} which was initially formulated for non-flat ray trajectories of plane waves propagated in a locally isotropic nonuniform medium. The formalism of ray trajectories is not applicable for a low-mode fiber. In this case, the rotation of the electric vector is characterized by parallel displacement of the state vector along the lines of energy flow mapped into a sphere in the pulse space. The direction of rotation of the electric vector is characterized by that of torsion of energy flow lines and is determined by the sign of the topological charge of the LV vortex.

One can excite a circularly polarized CP_{lm}^σ wave Eq. (30) with degenerated boundary dislocation in a fiber. Let us write the transversal electric field in the form

$$\mathbf{e}_1(CP_{lm}^{\sigma, \text{even}}) = \{\hat{\mathbf{x}} + i\sigma \hat{\mathbf{y}}\} \times \cos(\sigma l \varphi - \delta\beta_{21} z) F_l(R) \exp(i\tilde{\beta}' z). \quad (34)$$

It follows from Eq. (34) that, in propagation along a parabolic fiber, the axis of degenerated boundary dislocation of vortex superposition rotate by the angle

$$\chi = -\sigma \delta\beta_{21} z = -(2\pi/\lambda) \delta n_T z. \quad (35)$$

The rotation direction of the dislocation axis is opposite to that of linear polarization in the Rytov–Vladimirskii effect. Such a rotation of boundary dislocation is a waveguide exhibition of the optical Magnus effect (Ref. 25).

Rotation of a field is characterized by the efficient refraction index δn_T both in the waveguide Rytov–Vladimirskii effect³³ and the waveguide optical Magnus effect.³⁵ This phenomenon is equivalent to circular

birefringence of a medium. However, first, it is observed in a *locally isotropic* medium; second, the refraction index δn_T depends on the topological charge σl . So, the value δn_T can be characterized as topological birefringence. A similar phenomenon was already observed earlier in multimode fibers (Ref. 9).

5.3. Linear birefringence. Joint Rytov–Magnus effect

Azimuthally symmetric TE and TM modes in optical fibers can be united in fields of unstable $IV_{\sigma}^{-\sigma}$ vortices containing partial $|+1, -1\rangle$ and $|-1, +1\rangle$ vortices whose amplitude oscillates during wave propagation along the z axis.¹⁴ One can demonstrate that “force” lines of the azimuth and radial components of the Poynting vector \mathbf{P} for the CP_{11}^+ field are deformed during propagation in such a fiber and form the following pictures in the cross section of the fiber (Fig. 2).

The change of the form of the force lines of the CP_{11}^+ mode is caused by oscillation changes of the IV vortex field in which beatings arise between the fields of partial $|+1; -1\rangle$ and $|-1; +1\rangle$ vortices. As a result of these beatings, opposite topological charges are added alternately in the CP_{11}^+ field and either a homogeneous circularly polarized field with degenerated boundary dislocation $|0; +1\rangle$ or a linearly polarized field with purely helical dislocation $|+1; 0\rangle$ is formed.

It is evident that analogs of fields of CP_{11}^+ mode and LV_{11} vortex are formed in certain sections of a stepwise fiber, and directions of rotations of linear polarization and axes of boundary dislocation are opposite. The distance between these sections is equal to a quarter of the beating length Λ for a IV vortex.¹⁴ In the sections $z = 2n(\Lambda_{IV}/4)$ ($n = 0, 1, 2, \dots$) the angle of rotation of the boundary dislocation axis χ is described by the expression (34) and characterizes the waveguide optical Magnus effect. In the sections $z = (2C+1)\Lambda_{IV}/4$ the angle ψ of rotation of the linear polarization vector of the LV_{11} vortex is described by the expression (35) and represents the Rytov–Vladimirskii effect. At the intermediate lengths of the fiber, Rytov’s effect and the optical Magnus effect are observed simultaneously. Below we characterize this phenomenon as the joint Rytov–Magnus effect. This effect is connected both with linear birefringence of TE and TM modes and with circular birefringence of homogeneous and inhomogeneous vortices in an inhomogeneous medium of the fiber.

Note that in propagation of a wave there arises conversion of the spin \mathbf{S} and angular \mathbf{L} momenta between the states $|0; +1\rangle$ and $|+1; 0\rangle$. The phenomenon of conversion $\mathbf{L} \Leftrightarrow \mathbf{S}$ can be observed only in fields with topological charge $|\sigma l| = 1$.

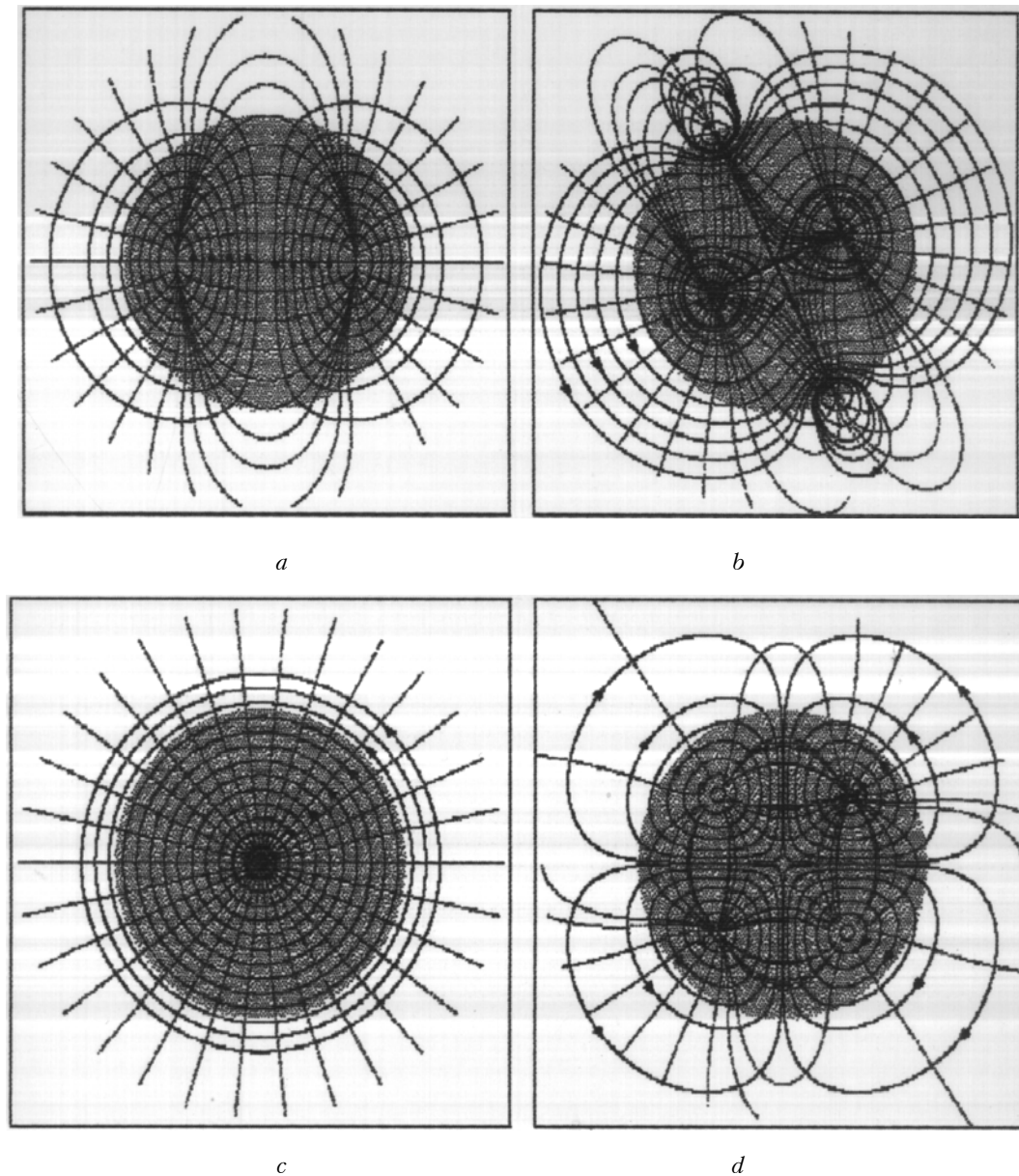


FIG. 2. The structure of force lines (lines with arrows) and pseudopotential lines of the transversal Poynting vector \mathbf{P}_\perp of a circularly polarized CP_{11} mode in the sections: $z=0$ (a); $z=\pi/(2(\beta_{TE}-\beta_{TM}))$ (b); $z=\pi/(\beta_{TE}-\beta_{TM})$ (c); lines of the vector \mathbf{P}_\perp of a linearly polarized LP_{11} mode (d). The painted circle means the core of a fiber with radius of $3.5 \mu\text{m}$.

6. THE EXPERIMENT

The experiment dealt with rotation of the direction of linear polarization ψ and axis of degenerated boundary dislocation χ in different sections of a fiber exciting it by a circularly polarized CP_{11}^+ mode (or a LV_{11} vortex). A low-mode optical fiber with stepwise profile of the refractive index was chosen. The permissible value of induced linear birefringence was $\delta n_L \sim 10^{-6}$. The radius of the fiber core was $\rho = 3.5 \mu\text{m}$, the waveguide parameter $V = 3.6$ for $\lambda = 0.63 \mu\text{m}$. The fiber could realize HE_{11} mode, CV_σ^σ and $IV_\sigma^{-\sigma}$ vortices. The experimental unit is presented in Fig. 3.

To suppress excitation of the HE_{11} mode maximally, a field of a circularly polarized CP_{11}^+ mode was formed at the exit of the fiber by use of a computer hologram. Fiber length was varied by truncating fiber parts of length of approximately 1 cm. Radiation from the exit end of the fiber was led by a $20\times$ microobjective and projected onto a screen. We measured value and sign of rotation angles of linear polarization ψ and axis of degenerated boundary dislocation χ .

Figure 4 presents the sequence of photo pictures of the near radiation field from the end of the fiber. The interference experiment detected a topological charge $|\sigma|=1$ in fields with pronounced central minimum of intensity.

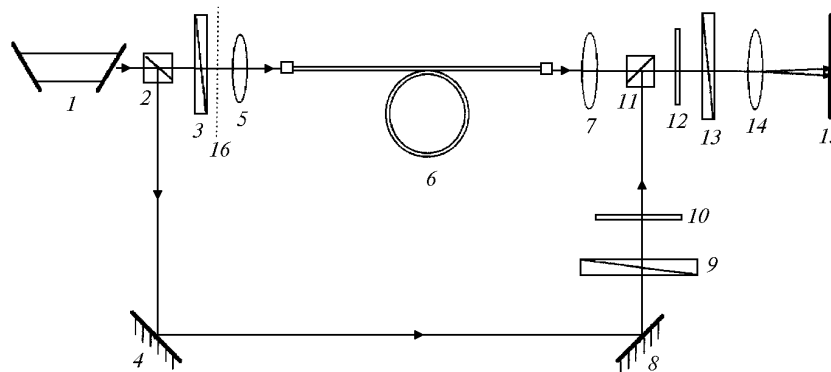


FIG. 3. The experimental unit for studying the CP_{11} mode: He-Ne laser (1); dividing prism (2, 11); polarizer (3, 9, 13); mirror (4, 8); $20\times$ microobjective (5,7); low-mode fiber (6); slab $\lambda/4$ (10, 12); lens (14); screen (15); computer hologram (16).

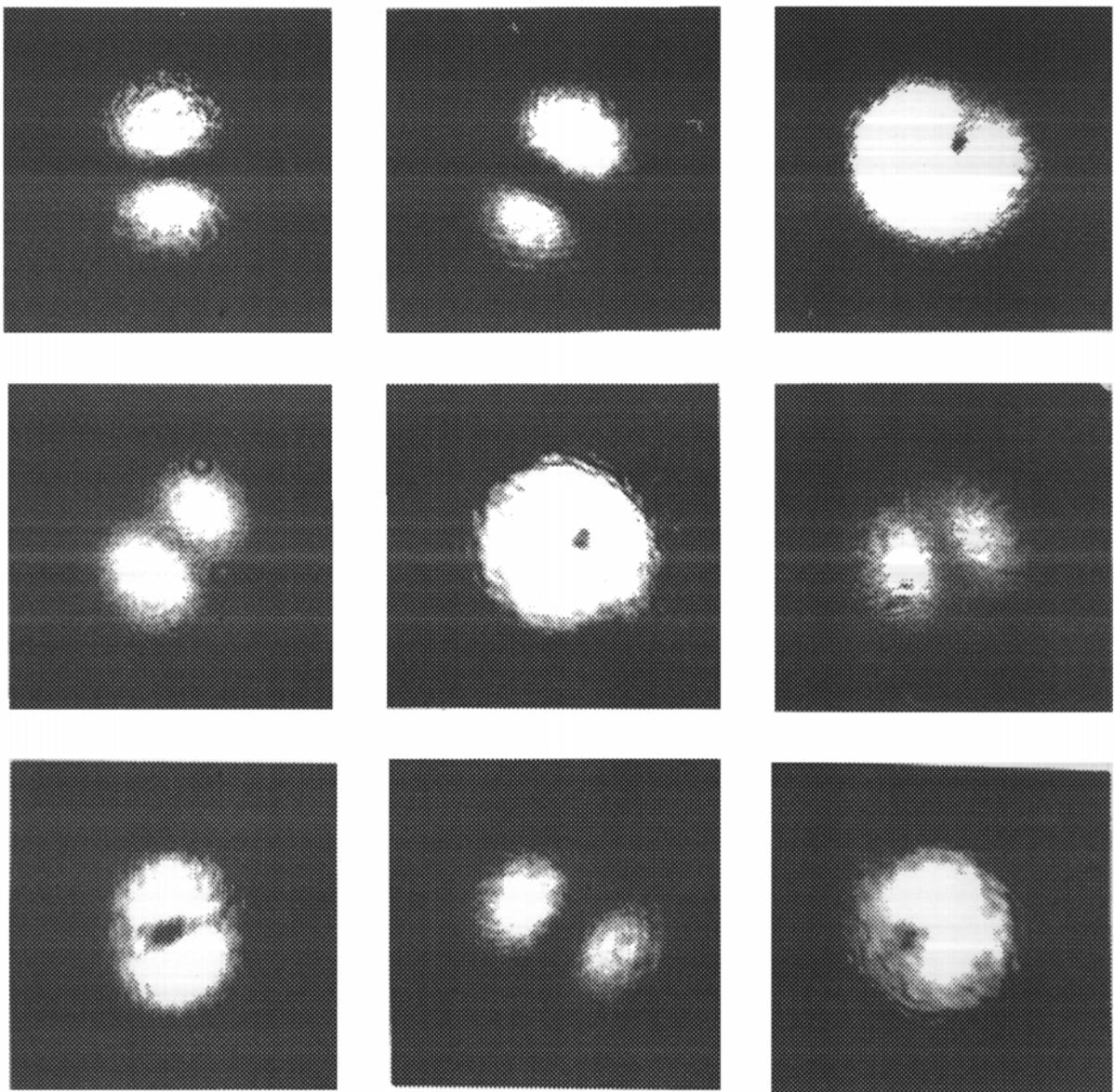


FIG. 4. Photo pictures of the near radiation field of a low-mode fiber in the generalized Rytov-Magnus effect.

Figure 5 presents the plots of rotation angles of the axis of degenerated boundary dislocation χ and azimuth of linear polarization ψ as functions of fiber length z .

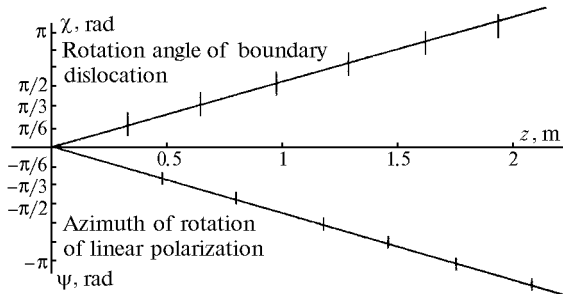


FIG. 5. Rotation angle of azimuth of linear polarization ψ and that of the axis of boundary dislocation χ in the radiation field of the CP_{11} mode as functions of length z : $\rho = 3.5 \mu\text{m}$; $n_{\text{co}} = 1.48$; $V = 3.6$; $\Delta \approx 10^{-3}$; $\lambda = 0.63 \mu\text{m}$.

If the fiber is excited by a LV vortex with $\sigma l = +1$, purely helical dislocations detected in the radiation field are also exclusively with $\sigma l = +1$. Similarly, with exciting the fiber by a right circularly polarized CP_{11} mode with $\sigma = +1$, only helical dislocations with $\sigma l = +1$ are detected in the radiation field. And otherwise, with exciting the fiber by a LV vortex with $\sigma l = -1$ (or a CP mode with $\sigma = -1$), only helical dislocations with $\sigma l = -1$ are detected.

As it was just supposed theoretically, the values of the angle of linear polarization ψ and angle χ of rotation of the axis of boundary dislocation linearly depend on the length z within the experimental error, but have opposite signs (see Eqs. (32) and (35)). The experiment yields the value of topological birefringence equal to $\delta n_T = (2.3 \pm 0.08) \cdot 10^{-6}$ (the theoretical value of birefringence is $\delta n_T = 3 \cdot 10^{-6}$ what is obtained from Eqs. (32), (33), and (35)).

7. CONCLUSION

Circularly polarized homogeneous and inhomogeneous CV vortices and azimuthally symmetrical linearly polarized TE and TM modes are eigenmodes of optical multimode fibers. A pair of numbers, topological charge σl and polarization $\varkappa\sigma$, corresponds to each CV vortex and characterizes the state of the vortex: $|\sigma l, \varkappa\sigma\rangle$. TE and TM modes are represented by connected vortices $|+1, -1\rangle \pm |-1, +1\rangle$. Each of these partial vortices cannot exist independently.

The propagation constant of an optical vortex in the free space is fourfold degenerated with respect to the topological charge l and circulation of wave polarization σ_z . In the medium of a low-mode fiber, the line of the propagation constant is split in the proper vortex due to spin-orbit interaction. This

corresponds to generation of homogeneous $CV_{\sigma l}^{\sigma}$ and inhomogeneous $CV_{\sigma l}^{\sigma}$ vortices. The value of the

propagation constant splitting $\tilde{\beta}$ is determined by the polarization correction $\delta\beta$. The vortex propagation constants are twofold degenerated with respect to l and σ .

The splitting of propagation constants $\tilde{\beta}$ is caused by accumulation of the Berry phase. In its turn, the topological phase γ_T represents the result of parallel displacement along the line of energy flow of a directed vortex mapped onto a sphere in the pulse space. Besides, the topological phase γ_T can be considered as a result of spin-orbit interaction in the field of an optical vortex. The process of this spin-orbit interaction is characterized by the operator \hat{V} whose mean physical value equals to the polarization correction $\delta\tilde{\beta}$ to the propagation constant $\tilde{\beta}$ proportionally to proper time of the directed vortex and depends on distribution form of the refractive index $n^2(R)$ of a low-mode fiber.

Spin-orbit interaction is selective in its action upon the fields of CV vortices and causes circular birefringence δn_C . Linear birefringence δn_L which is characterized by the polarization correction $\beta^{(1)}$ arises in the fields of TE and TM modes. In gradient fibers, the orders of circular and linear birefringence are as follows: $\delta n_C \sim (\lambda/\rho)$ and $\delta n_L \sim (\lambda/\rho)^3$, respectively (ρ is the fiber radius). The orders of δn_C and δn_L are similar in stepwise fibers.

To characterize birefringence in crystals, it is sufficient to assign the basis of wave polarization. As for a locally isotropic medium of optical fibers, it is necessary to assign the topological charge σl together with the polarization basis $\varkappa\sigma$.

In fibers, circular and linear birefringence can act simultaneously and are united by a common term, namely, topological birefringence. Experimentally, topological birefringence is exhibited as the joint Rytov–Magnus effect. Structural instability of an IV vortex is also a result of linear birefringence in fibers.

ACKNOWLEDGMENTS

The results of this work were reported and discussed at the First International Conference on Singular Optics–97 (Ukraine, Crimea, Partenit, October 1997). The authors are thankful to M. Berry for notes on the problem of the topological phase, to K.N. Alekseev and Yu.N. Fridman for consultations on the problem of the operator of spin-orbit interaction.

REFERENCES

1. L. Allen, W. Beijersbergen, R.J.C. Spreeuw, and J.P. Woerdvan, Phys. Rev. **A45**, No. 11, 8185–8189 (1992).

2. S.M. Barnett and L. Allen, *Opt. Commun.* **110**, 670–678 (1994).
3. L.D. Landau and E.M. Lifshits, *Theoretical Physics*, (Nauka, Moscow, 1989), vol. III, 768 pp.
4. M.V. Berry, *Proc. Roy. Soc. Lond.* **A392**, 45–47 (1984).
5. A.V. Volyar, N.V. Kukhtarev, S.N. Lapaeva, and P.N. Leifer, *Pis'ma Zh. Tekh. Fiz.* **17**, No. 13, 1–5 (1991).
6. S.M. Rytov, *Dokl. Akad. Nauk SSSR* **28**, 263 (1938).
7. V.V. Vladimirkii, *Dokl. Akad. Nauk SSSR* **31**, 222 (1940).
8. A.V. Volyar, A.V. Granovskii, V.I. Myagkov, and S.N. Lapaeva, *Ukr. Fiz. Zh.* **37**, No. 10, 1468–1471 (1992).
9. A.V. Volyar, Yu.N. Mitsai, V.I. Myagkov, and T.A. Fadeeva, *Pis'ma Zh. Tekh. Fiz.* **20**, No. 3, 48–52 (1994).
10. D. Gloge and D. Marcuse, *J. Opt. Soc. Am.* **59**, No. 12, 1629–1631 (1969).
11. G. Eichmann, *JOSA* **61**, No. 2, 161–168 (1970).
12. V.S. Liberman and B.Ya. Zel'dovich, *Phys. Rev.* **A46**, No. 8, 5199–5207 (1992).
13. A.W. Snyder and J.D. Love, *Optical Waveguide Theory* (Chapman and Hall, London–New York, 1983).
14. A.V. Volyar and T.A. Fadeeva, *Opt. Spektrosk.* (in print).
15. A.S. Davydov, *Quantum Mechanics* (Nauka, Moscow, 1976), 703 pp.
16. S. Pancharatnam, *Proc. Ind. Acad. Sci.* **A44**, 247–260 (1956).
17. E. Abramochkin and V. Volostnikov, *Opt. Comm.* **83**, No. 12, 123–135 (1991).
18. M. Stone and W.E. Goff, *Nuclear Phys.* **B295**, 243–261 (1988).
19. A.V. Volyar and T.A. Fadeeva, *Pis'ma Zh. Tekh. Fiz.* **22**, No. 8, 57–62 (1996).
20. M.Ya. Darsht, B.Ya. Zel'dovich, I.V. Kataevskaya, and N.D. Kundikova, *Zh. Eksp. Teor. Fiz.*, No. 6, 1464–1472 (1995).
21. E. Born and M. Wolf, *Principles of Optics* (Pergamon Press, Oxford, 1970).
22. V.S. Liberman and B.Ya. Zel'dovich, *Phys. Rev.* **E49**, No. 3, 2389–2396 (1994).
23. A.Yu. Savchenko and B.Ya. Zel'dovich, *Phys. Rev.* **E50**, No. 3, 2287–2292 (1994).
24. A.V. Volyar and T.A. Fadeeva, *Pis'ma Zh. Tekh. Fiz.* **22**, No. 8, 63–67 (1996).
25. A.V. Volyar and S.N. Lapaeva, *Pis'ma Zh. Tekh. Fiz.* **18**, No. 24, 74–77 (1992).